Contents lists available at ScienceDirect

Food Research International

journal homepage: www.elsevier.com

Colloidal properties of sodium caseinate-stabilized nanoemulsions prepared by a combination of a high-energy homogenization and evaporative ripening methods

J.M. Montes de Oca-Ávalos[a], R.J. Candal[b], M.L. Herrera[a,*]

[a] Institute of Polymer Technology and Nanotechnology, University of Buenos Aires-CONICET, Faculty of Engineering, Las Heras 2214, C1127AAQ Ciudad de Buenos Aires, Argentina
[b] Instituto de Investigación e Ingeniería Ambiental, Universidad Nacional de San Martín (UNSAM), Campus Miguelete, 25 de Mayo y Francia, 1650 San Martín, Provincia de Buenos Aires, Argentina

ARTICLE INFO

Chemical compounds studied in this article:
Casein (PubChem CID: 73995022)
Sucrose (PubChem CID: 5988)
Ethyl acetate (PubChem CID: 8857)

Keywords:
Nanoemulsions
Sodium caseinate
Droplet size
Zeta potential
Stability
Structure

ABSTRACT

Nanoemulsions stabilized by sodium caseinate (NaCas) were prepared using a combination of a high-energy homogenization and evaporative ripening methods. The effects of protein concentration and sucrose addition on physical properties were analyzed by dynamic light scattering (DLS), Turbiscan analysis, confocal laser scanning microscopy (CLSM) and small angle X-ray scattering (SAXS). Droplets sizes were smaller (~ 100 nm in diameter) than the ones obtained by other methods (200 to 2000 nm in diameter). The stability behavior was also different. These emulsions were not destabilized by creaming. As droplets were so small, gravitational forces were negligible. On the contrary, when they showed destabilization the main mechanism was flocculation. Stability of nanoemulsions increased with increasing protein concentrations. Nanoemulsions with 3 or 4 wt% NaCas were slightly turbid systems that remained stable for at least two months. According to SAXS and Turbiscan results, aggregates remained in the nano range showing small tendency to aggregation. In those systems, interactive forces were weak due to the small diameter of flocs.

1. Introduction

Nanoemulsions are defined as a thermodynamically unstable colloidal dispersion with a dispersed phase containing small spherical droplets with radius sizes smaller than 100 nm (McClements, 2012a). A conventional emulsion typically has particles with mean radii between 100 nm and 100 μm (McClements & Rao, 2011). Both conventional emulsions and nanoemulsions are metastable systems that break due to a variety of destabilization mechanisms, such as gravitational separation, coalescence, flocculation, and Ostwald ripening (Komaiko & McClements, 2016). For certain applications, it is desirable to prepare systems with very small particles since they have a number of potential advantages over systems containing larger particles (Fryd & Mason, 2012). First, they usually have better stability to physical changes, and second, they contain particles that only scatter light waves weakly, and so they are suitable for incorporation into products that need to be optically clear or only slightly turbid (McClements, 2012b). Nanoemulsions also enhance bioavailability and because of that have been used in many applications involving encapsulation of bioactive compounds (Atrux-Tallau, Lasselin, Han, Delmas, & Bibette, 2014; Komaiko, Sastrosubroto, & McClements, 2016; Vilanova & Solans, 2015).

Nanoemulsions have been prepared by high-energy and low-energy homogenization methods (Silva, Cerqueira, & Vicente, 2012). High-energy methods (such as high-pressure homogenization, microfluidization or sonication) often require a large capital investment in equipment while the major disadvantage for the low-energy methods (such as phase inversion temperature, spontaneous emulsification, or emulsion phase inversion) is the requirement of high amounts of synthetic surfactants (Komaiko & McClements, 2016). Low-energy methods are often more effective at producing small droplet sizes than high-energy approaches, but they are often more limited in the types of oils and emulsifiers that can be used. For example, it is currently not possible to use proteins or polysaccharides as emulsifiers in most of the low-energy approaches used to form nanoemulsions (McClements & Rao, 2011). Although both, high-energy and low-energy homogenization methods have drawbacks, they enable preparing extremely fine particulate nanodispersions when the stabilizer is a small-molecule surfactant (Chu, Ichikawa, Kanafusa, & Nakajima, 2007). In protein systems, a

Abbreviations: NaCas, sodium caseinate; DLS, dynamic light scattering; SLS, static light scattering; CLSM, confocal laser scanning microscopy; SAXS, small angle X-ray scattering.

* Corresponding author.
Email address: mlidiaherrera@gmail.com (M.L. Herrera)

http://dx.doi.org/10.1016/j.foodres.2017.06.035
Received 31 March 2017; Received in revised form 13 June 2017; Accepted 17 June 2017
Available online xxx
0963-9969/

combination of high-energy homogenization and evaporative ripening methods was used to prepare nanoemulsions formulated with corn oil and whey protein (Lee & McClements, 2010). The application of nanotechnology to the food field may allow modifying macroscale properties such as texture, transparency, and stability during shelf life among other characteristics. Therefore, it is of great interest to study physical properties of nanosystems.

Nanoemulsions have been used for applications in the food industry such as beverage (Rao & McClements, 2013; Zhang, Hayes, Chen, & Zhong, 2013; Zhang, Peppard, & Reineccius, 2015), healthier ice cream, frozen food or they have been designed for performing as carriers or delivery systems for lipophilic compounds (Gulotta, Saberi, Nicoli, & McClements, 2014; Silva et al., 2012). Recently, formulation of food grade O/W nanoemulsions has been an area of active research (Hategekimana, Chamba, Shoemaker, Majeed, & Zhong, 2015; Komaiko et al., 2016; McClements & Rao, 2011; Ozturk, Argin, Ozilgen, & McClements, 2015; Tabibiazar & Hamishehkar, 2015), to name a few. Dairy proteins have been extensively used as emulsifiers in conventional emulsions since they adsorb to the oil droplet interface, forming a strong and cohesive protective film that helps prevent droplet aggregation. Sodium caseinate is widely used as an ingredient in the food industry due to its functional properties, which include emulsification, water and fat-binding, thickening and gelation. Maher, Fenelon, Zhou, Haque, and Roos (2011) prepared microfluidized nanoemulsions stabilized by sodium caseinate with droplet sizes between 186 and 199 nm (around 200 nm). Yeramilli and Ghosh used high-pressure homogenizer, obtaining droplets within the same size. In this article, we prepared nanoemulsions using a combination of methods with the aim of obtaining smaller droplets than in Maher et al. (2011) or in Yeramilli and Ghosh (2017) articles. The physical behavior of systems with droplets smaller than 200 nm is expected to be different than the one reported in literature and therefore it is interesting to explore their stability and structure.

The objective of the present study was to investigate the formation of sodium caseinate-stabilized nanoemulsions using a combination of a high-energy homogenization and evaporative ripening methods. The effects of protein concentration and sucrose addition on physical properties were analyzed by dynamic light scattering (DLS), Turbiscan analysis, confocal laser scanning microscopy (CLSM) and small angle X-ray scattering (SAXS) with the aim of describing in a deeper way the stability behavior.

2. Materials and methods

2.1. Materials

Sucrose (α-D-glucopyranosyl β-D-fructofuranoside) and sodium caseinate (NaCas) were obtained from Sigma (Sigma–Aldrich, St. Louis, Mo., USA) and ethyl acetate from Sintorgan (Sintorgan S.A., Buenos Aires, Argentina). All reagents were analytical grade and they were used without any further purification. HPLC water was used for all experimental work. The oil phase was commercial sunflower seed oil (SFO) which main fatty acids were identified as C16:0 (palmitic), C18:0 (stearic), C18:1 (*cis*, oleic), and C18:2 (*cis*, linoleic) with percentages of 6.4%, 3.8%, 20.7%, and 67.6%, respectively.

2.2. Emulsion preparation

Nanoemulsions were prepared using a combination of a high-energy homogenization and evaporative ripening methods previously reported for whey protein-stabilized systems with some minor changes (Lee & McClements, 2010). Oil phase was a blend of commercial SFO (15 wt%) and ethyl acetate (85 wt%). In all nanoemulsions the ratio NaCas/SFO was 0.6. Aqueous phase contained sucrose in concentrations of 0, 2, 4, 6, or 8 wt% and NaCas in concentrations of 1.0, 2.0, 3.0, or 4.0 wt%. Sodium caseinate was slowly added to water under constant stirring. Samples were kept overnight to dissolve protein. Weights of all components, expressed in grams per 100 g of nanoemulsion are reported in Table 1. Sodium azide was used in a percentage of 0.01% to prevent microbial contamination. Oil and aqueous phases were mixed using an Ultra-Turrax (UT) T8 high speed blender (S 8N-5G dispersing tool, IKA Labortechnik, Janke& Kunkel, GmbH & Co., Staufen, Germany), operated at 20,000 rpm for 1 min. Samples were kept in an ice bath (0 °C) during processing. Coarse emulsions were obtained after repeating this process three times. The resultant coarse emulsions were further homogenized for 20 min using an ultrasonic liquid processing (US), VIBRA CELL, VC750 (power 750 W, frequency 20 kHz) model (Sonics & Materials, Inc., Newtown, CT, USA), with a 13-mm-diameter and 136-mm-length tip and an amplitude of 30%. The temperature of the sample-cell was controlled by means of an ice bath (0 °C) with a temperature cut down control of 20 ± 1 °C during ultrasound treatment. After ultrasound treatment, fine emulsions were obtained, but they were still conventional emulsions. Fine emulsions were placed in a rotary evaporator Buchi model R 100 (Buchi, Postfach, Switzerland) connected to a vacuum pump and a recirculating chiller to eliminate ethyl acetate. The degree of ethyl acetate evaporation was determined by carrying out a mass balance of emulsions before and after solvent evaporation. The process was performed at 45 °C for 20 min. After evaporation, enough amount of water was added to the samples in order to keep constant the composition of aqueous phase. Then, the samples were cooled quiescently to ambient temperature (22.5 °C). Subsequently they were analyzed for particle size distribution, zeta potential (ζ), stability in quiescent conditions and microstructure. The pHs of the SFO emulsions were 6.66 ± 0.05. No buffer was added to the emulsions. Experiments were done in duplicate and results were averaged.

2.3. Particle size distribution, polydispersity, and zeta potential

Nanoemulsions immediately after preparation and after 3 days of storage at 22.5 °C were characterized with respect to volume distributions of droplets and the zeta potential (ζ-potential) by dynamic light scattering (DLS). The average diameter of droplets (Z-average), the width of the droplet distribution, indicated by the polydispersity index (PDI), and the ζ-potential were measured using a DLS device

Table 1
Final composition for nanoemulsions prepared by a combination of high-energy homogenization/evaporative ripening methods.

Nanoemulsion name	Sodium caseinate (NaCas, wt%)	Sucrose (S, wt%)	Sunflower oil (SFO, wt%)
1 NaCas 0 S	0.98	0	1.64
1 NaCas 2 S	0.98	1.97	1.64
1 NaCas 4 S	0.98	3.93	1.64
1 NaCas 6 S	0.98	5.90	1.64
1 NaCas 8 S	0.98	7.87	1.64
2 NaCas 0 S	1.94	0	3.23
2 NaCas 2 S	1.94	1.94	3.23
2 NaCas 4 S	1.94	3.87	3.23
2 NaCas 6 S	1.94	5.81	3.23
2 NaCas 8 S	1.94	7.74	3.23
3 NaCas 0 S	2.86	0	4.76
3 NaCas 2 S	2.86	1.90	4.76
3 NaCas 4 S	2.86	3.81	4.76
3 NaCas 6 S	2.86	5.71	4.76
3 NaCas 8 S	2.86	7.62	4.76
4 NaCas 0 S	3.75	0	6.25
4 NaCas 2 S	3.75	1.88	6.25
4 NaCas 4 S	3.75	3.75	6.25
4 NaCas 6 S	3.75	5.63	6.25
4 NaCas 8 S	3.75	7.50	6.25

NanoBrook 90Plus Particle Size Analyzer (Brookhaven Instruments Corporation, New York, USA) equipped with a laser and operated at room temperature. During the whole sets of experiments, the nanoemulsions were diluted until the final concentration of NaCas was 0.1 wt%. The measurements were performed in duplicate with a scattering angle of 90°. For ζ-potential experiments, KCl was added to reach a final concentration of 1 mM.

To analyze emulsions with droplet sizes > 3 μm or to check the absence of these big droplets in the nanoemulsions, droplet size distribution of all samples was also measured by static light scattering (SLS) using a Mastersizer 2000 with a Hydro 2000MU as dispersion unit (Malvern Instruments Ltd., UK). The pump speed was settled at 1800 RPM. Refraction index for the oil phase was 1.4694. Determinations were conducted in duplicate and values of standard deviations were < 0.2 μm. Distributions were expressed as differential volume. Parameters selected to describe the distributions were volume-weighted mean diameter ($D_{4,3}$), distribution width (W), and volume percentage of particles exceeding 1 μm in diameter (%V_d > 1) (Thanasukarn, Pongsawatmanit, & McClements, 2006).

2.4. Stability by Turbiscan

The stability of the emulsions was analyzed using a vertical scan analyzer Turbiscan MA 2000 (Formulaction, Toulouse, France). A scheme of the equipment was reported in Pan, Tomás, and Añón (2002). Briefly, the reading head is composed of a pulsed near-IR light source (λ = 850 nm) and two synchronous detectors. The transmission detector receives the light, which goes through the sample (0°), while the back-scattering detector receives the light back-scattered by the sample (135°). The samples were placed in a flat-bottomed cylindrical glass measurement cell and scanned from the bottom to the top in order to monitor the optical properties of the dispersion along the height of the sample in the cell. The backscattering (BS) and transmission (T) profiles as a function of the sample height (total height = 60 mm) were studied in quiescent conditions at 22.5 °C. Measurements of the emulsions were performed immediately after preparation and once a day during two months. Experiments were done in duplicate and standard deviation for BS differed by < 0.2% for all samples. The mechanism making the dispersion unstable was deduced from the transmission or the backscattering data. For flocculation kinetics, the BS profiles were expressed in reference mode ($\Delta BS = BS_t - BS_{0,}$ with BS_t, the BS at time t, and BS_0, the BS at t = 0). The Average Back Scattering (BS_{av}) was calculated in the 20–50 mm zone since this is the region no affected by creaming (bottom and top of the tube, Álvarez Cerimedo, Huck Iriart, Candal, & Herrera, 2010; Mengual, Meunier, Cayre, Puech, & Snabre, 1999).

2.5. Nanoemulsions structure by CLSM

The Olympus FV300 (Olympus Ltd., London, UK) confocal laser scanning microscope (CLSM) with an Ar gas laser (k = 488 nm) was used to collect the images. A 10 × ocular was used, together with a 60 × objective for a visual magnification of 600 ×. The laser intensity used was below 10% to avoid photochemical decomposition of the Nile-Red colorant (Sigma Aldrich St. Louis, Mo., USA). Images were recorded by using confocal assistant Olympus Fluoview version 3.3 software provided with the FV300 CLSM. All samples were kept at 22.5 °C for 24 h before observation.

2.6. Nanoemulsions structure by SAXS

The SAXS measurements were performed at the DO2A-SAXS1beamline of the Synchrotron National Laboratory (LNLS, Campinas, Brazil) with a 1.548 Å wavelength. The scattering intensity distributions as a function of scattering vector q were obtained in the q range between 0.035 and 1.33 nm^{-1}, with $q = (4\pi / \lambda) \sin(\theta)$, where λ is the radiation wavelength and 2θ is the scattering angle. The SAXS patterns were recorded with exposure times of 1 min. A Pilatus 300 K detector was used with 3090.7 mm sample detector distance. One-dimensional curves were obtained by integration of the 2D data using the program FIT-2D (Hammersley, Svernsson, Hanfland, Fitch, & Häusermann, 1996). All emulsion systems were kept at 22.5 °C. Then, they were placed in the beamline vacuum-tight temperature-controlled X-ray cell for liquids (Cavalcanti et al., 2004) maintained at the same temperature. The SAXS normalized patterns were evaluated to obtain q_{max} values for peaks of intensity vs. q curves.

2.7. Statistical analysis

For DLS, SLS and Turbiscan data, significant differences between means were determined by the Student's *t*-test. An α level of 0.05 was used for significance. Results are reported as mean and standard deviation.

3. Results and discussion

3.1. Droplet size distribution

To check the ability of the combination of high-energy homogenization and evaporative ripening methods to produce nanoemulsions, samples were analyzed for particle size distribution after ultrasound treatment and after evaporative step. Fig. 1 shows the droplet size distributions of fine emulsions before applying the evaporative step while Fig. 2 reports the same emulsions after evaporating ethyl acetate. Figs. 1a and 2a show the effect of NaCas concentration and Figs. 1b and 2b report the effect of sucrose on the 4 wt% NaCas system. Parameters of distributions shown in Fig. 1 were summarized in Table 2. Most emulsions showed three populations after ultrasound treatment (Fig. 1): Two big populations with smaller $D_{4,3}$ and a third small population at greater $D_{4,3}$. There were no significant differences among distributions parameters for NaCas concentrations of 1, 2 and 3 wt% (Table 2). Slightly significant differences in distribution parameters were found between 1, 2, or 3 wt% and 4 wt% NaCas concentration (Table 2). This protein amount improved droplet size distribution in terms of droplet sizes and width of the distribution. Besides, distributions became almost monomodal with a small population at greater $D_{4,3}$ by addition of 4 wt% or more sucrose. Table 2 showed that addition of 4 wt% or more sucrose slightly decreased $D_{4,3}$ ($p < 0.05$). $D_{4,3}$ of samples reported in Fig. 1 varied from 480 to 680 nm. The evaporative ripening step clearly helps reducing droplet size (Fig. 2). Besides, after addition of one more step in preparation, the evaporative step, distributions became monomodal. Fig. 2 also shows that distribution width significantly decreased after evaporative step. All distributions in Fig. 2 were narrower than in Fig. 1. Table 3 summarizes average droplet size (Z-average) of distributions in volume and polydispersity index (PDI) for all emulsions reported in Fig. 2. Z-average varied from 89 to 120 nm. Lee and McClements (2010) used the combination of these methods to prepare nanoemulsions using food grade ingredients (corn oil, whey protein, and water). According to these authors, the droplets in the emulsions should shrink when ethyl acetate is removed from them due to evaporation. In addition, in their systems droplet size reduction increased when ethyl acetate content in the organic phase increased. Emulsions were all monomodal for all concentrations of solvent. However, the peak of the distribution was at smaller particle diameters for emulsions containing higher amounts of ethyl acetate. The results obtained in our systems agree with the behavior predicted for Lee and McClements (2010). In this study we selected a fixed ratio NaCas/SFO.

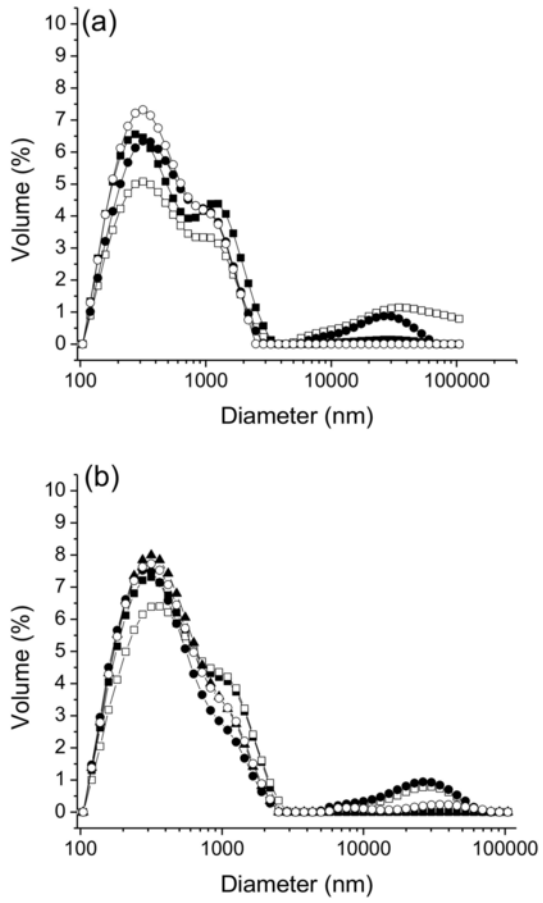

Fig. 1. Particle size distributions of fine emulsions obtained before applying evaporative ripening method. a) Different concentrations of NaCas: 1 (■), 2 (□), 3 (●) and 4 (○) wt%; b) 4 wt%. NaCas and different sucrose concentrations: 0 (■), 2 (□), 4 (●), 6 (○), and 8 (▲) wt%.

As ethyl acetate was in all emulsions 85 wt% of oil phase, droplet reduction was similar, around five times, for all emulsions prepared. In all formulations studied, combination of methods allows obtaining nanoemulsions with a PDI close to 25%. Troncoso, Aguilera, and McClements (2012) prepared Tween 20-stabilized O/W nanoemulsions using corn oil as fat phase and hexane as solvent. According to these authors, the quality of a colloidal dispersion can be quantified in terms of its PDI. For Tween 20 nanoemulsions it varied from 4 to 12%, which indicated a good monodispersity of the samples. NaCas produced lower quality nanoemulsions than a non-ionic surfactant but they were still monomodal systems.

To analyze nanoemulsions physical stability, particle size distributions were measured after 72 h of storage at 22.5 °C. No significant differences in Z-average or PDI between nanoemulsions immediately after preparation and stored nanoemulsions were found (data not shown). These results indicated that all nanoemulsions were stable systems. When conventional emulsions with similar formulations were analyzed, they showed changes in 72 h and behaved as unstable systems (Álvarez Cerimedo et al., 2010). Thus, droplet sizes prove to be very relevant to stability.

3.2. Zeta potential

The electrical charge on oil droplets surface in the nanoemulsions was quantified measuring the ζ-potential of droplets obtained after ethyl acetate evaporation. Fig. 3 reports results for nanoemulsions immediately after preparation and nanoemulsions stored for 3 days at

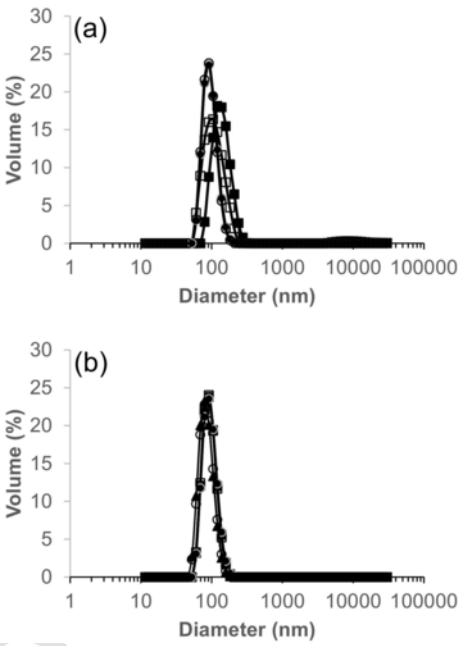

Fig. 2. Particle size distributions of emulsions obtained after combining a high-energy homogenization and evaporative ripening methods. a) Different concentrations of NaCas: 1 (■), 2 (□), 3 (●), and 4 (○) wt%; b) 4 wt% NaCas and different sucrose concentrations: 0 (■), 2 (□), 4 (●), 6 (○) and 8 (▲) wt%.

Table 2
Volume-weighted mean diameter ($D_{4,3}$, μm), width of the distribution (W), and volume percentage of particles exceeding 1 μm in diameter ($\%V_{d>1}$) of conventional emulsions reported in Fig. 1.

Emulsion	$D_{4,3}$ (μm)	W (μm)	$\%V_{d>1}$
NaCas			
1 wt%	0.68 ± 0.03^{a}	1.64 ± 0.28^{a}	24.0 ± 1.1^{a}
2 wt%	0.64 ± 0.06^{a}	1.56 ± 0.21^{a}	25.9 ± 0.3^{a}
3 wt%	0.62 ± 0.02^{a}	1.71 ± 0.33^{a}	25.1 ± 0.1^{a}
4 wt%	0.57 ± 0.01^{b}	0.99 ± 0.21^{b}	22.6 ± 0.1^{b}
NaCas 4 wt% sucrose			
2 wt%	0.59 ± 0.03^{a}	1.01 ± 0.01^{a}	22.0 ± 0.7^{a}
4 wt%	0.51 ± 0.01^{b}	0.82 ± 0.01^{b}	10.6 ± 0.1^{b}
6 wt%	0.48 ± 0.03^{b}	0.64 ± 0.01^{c}	8.0 ± 0.1^{c}
8 wt%	0.51 ± 0.02^{b}	0.65 ± 0.05^{c}	3.6 ± 1.0^{d}

Significant differences between means were determined by the Student's *t*-test with an α level of 0.05. Data in the same column with the same superscript are not significantly different.

22.5 °C. In all cases, the nanoemulsion droplets were negatively charged because pH was close to 7, above protein isoelectric point. For all nanoemulsions, the initial ζ-potential values indicated strong electrostatic repulsion of the dispersed oil droplets in the aqueous phase leading to good stability. The ζ-potential did not show significant differences for different NaCas or sucrose concentrations ($p < 0.05$). In our emulsions, the ζ-potential was independent of particle size. No significant differences were found between nanoemulsions immediately after preparation and after three days of storage indicating that nanoemulsions remained stable during that period ($p < 0.05$).

3.3. Stability by Turbiscan

Fig. 4 reports BS profiles vs. tube length for nanoemulsions immediately after preparation. For nanoemulsions formulated without sucrose (Fig. 4a), BS increased when NaCas concentration increased. This was expected since as the ratio NaCas/SFO was fixed at 0.6, droplet concentration should be higher for 4 wt% than for 1 wt% NaCas. Most likely droplet concentration was the most important effect on BS. All concen-

Table 3
Average droplet size (Z-average, nm) of distribution in volume and polydispersity index (PDI) of nanoemulsions reported in Table 1.

Nanoemulsion	Z-average (nm)	PDI (%)
1 NaCas 0 S	119 ± 3^{a}	27 ± 2^{a}
1 NaCas 2 S	114 ± 2^{a}	27 ± 1^{a}
1 NaCas 4 S	119 ± 3^{a}	29 ± 2^{a}
1 NaCas 6 S	118 ± 4^{a}	27 ± 2^{a}
1 NaCas 8 S	120 ± 3^{a}	29 ± 2^{a}
2 NaCas 0 S	110 ± 7^{b}	29 ± 2^{a}
2 NaCas 2 S	114 ± 4^{b}	26 ± 2^{a}
2 NaCas 4 S	111 ± 3^{b}	25 ± 2^{a}
2 NaCas 6 S	107 ± 2^{b}	27 ± 2^{a}
2 NaCas 8 S	104 ± 2^{b}	27 ± 2^{a}
3 NaCas 0 S	101 ± 1^{b}	25 ± 2^{a}
3 NaCas 2 S	102 ± 2^{b}	25 ± 2^{a}
3 NaCas 4 S	100 ± 2^{b}	26 ± 1^{a}
3 NaCas 6 S	95 ± 1^{c}	25 ± 2^{a}
3 NaCas 8 S	98 ± 1^{b}	27 ± 2^{a}
4 NaCas 0 S	94 ± 1^{c}	22 ± 1^{b}
4 NaCas 2 S	95 ± 1^{c}	25 ± 2^{a}
4 NaCas 4 S	95 ± 2^{c}	25 ± 2^{a}
4 NaCas 6 S	89 ± 2^{d}	25 ± 2^{a}
4 NaCas 8 S	89 ± 1^{d}	22 ± 1^{b}

Significant differences between means were determined by the Student's *t*-test with an α level of 0.05. Data in the same column with the same superscript are not significantly different.

trations of NaCas selected showed BS lower than 18% indicating that emulsions were transparent or slightly turbid. Conventional emulsions with the same formulation as nanoemulsions had BS > 60%. They were turbid systems that did not transmit light. Addition of sucrose to the 4 wt% NaCas nanoemulsion diminished BS (Fig. 4b). The BS of nanoemulsions containing 8 wt% sucrose was significantly lower than for formulation without sucrose. This was in agreement with the fact that addition of sucrose to the 4 wt% NaCas-stabilized nanoemulsion slightly decreased z-average (Table 3).

Fig. 5 shows representative ΔBS profiles vs. tube length obtained at different times for the nanoemulsions formulated with 1 or 4 wt% NaCas without sugar or with addition of 8 wt% sucrose. Nanoemulsion formulated with 1 wt% NaCas and no sucrose added to the aqueous phase was stable for 7 days (Fig. 5a). During this period, no significant differences were found between BS_0 and BS_t ($p < 0.05$). Then, destabilization occurred by two mechanisms: sedimentation and flocculation. The latter was the main destabilization mechanism for this formulation. Sedimentation was evidenced by an increase in ΔBS at the bottom zone (0–20 mm). As the density of aggregates is higher than the one of continuous phase, it is likely that they were formed mainly by protein aggregates. Sedimentation started after a week but after two weeks the bottom zone (0–20 mm) of the profile showed no significant differences (light grey solid line) with the initial profile indicating that protein aggregates were re-dissolved. Even in quiescent conditions, aggregation was reversible. Migration of oil droplets due to gravitational force was negligible. This fact was not surprising considering the size of the droplets. Flocculation destabilization also started after 1 week as was evidenced by a significant increase in BS_{avt} (20–50 mm). After 2 months, BS_{avt} was 14% higher than BS_{av0}. For the sample formulated with 1 wt% NaCas and 8 wt% sucrose (Fig. 5b), the behavior was similar. No significant differences in flocculation kinetics for addition of sucrose were found. This sample also showed sedimentation as secondary

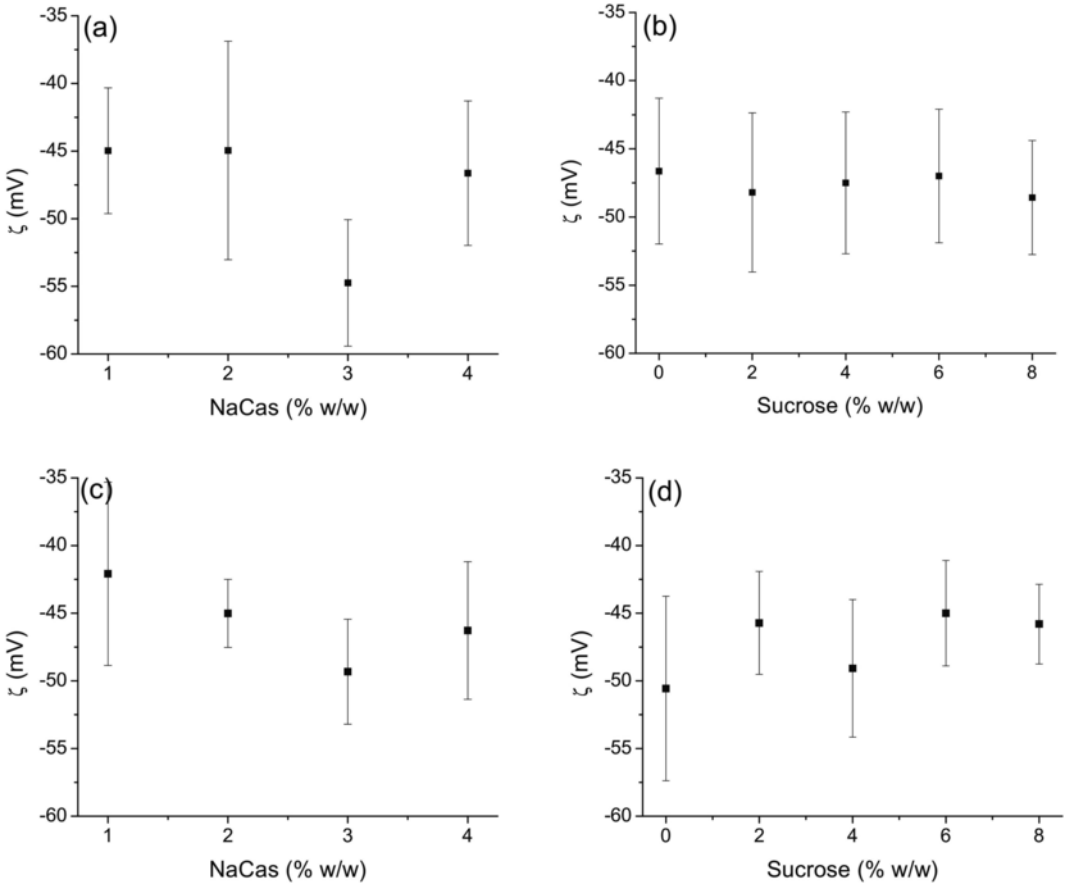

Fig. 3. The ζ-potential of droplets obtained after ethyl acetate evaporation for nanoemulsions immediately after preparation: a) NaCas concentrations ranging from 1 to 4 wt% b) 4 wt% NaCas and sucrose concentrations from 0 to 8 wt%; and for nanoemulsions after 3 days of storage at 22.5 °C: c) NaCas concentrations ranging from 1 to 4 wt%, b) 4 wt% NaCas and 0 to 8 wt% sucrose.

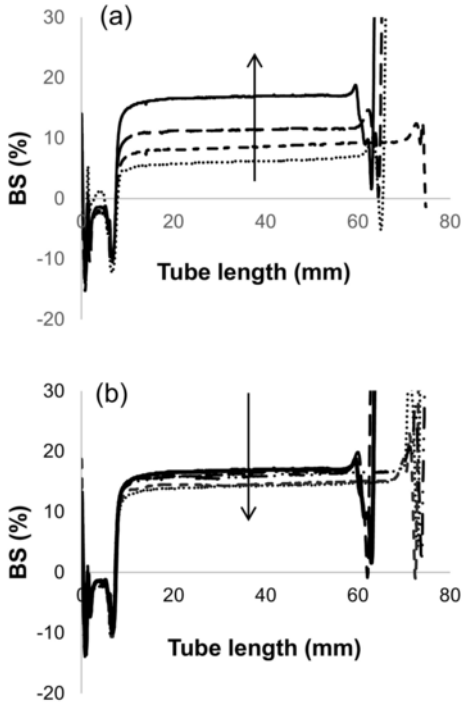

Fig. 4. Back scattering (BS) profiles obtained immediately after emulsions preparation. (a) Different sodium caseinate concentrations (NaCas): (....) 1 wt%, (- - -) 2 wt%, (— —) 3 wt%, (___) 4 wt%. (b) 4 wt% NaCas and different sucrose concentrations: (___) 0 wt%, (— ——) 2 wt%, (— . .) 4 wt%, (- - -) 6 wt%, (....) 8 wt%. Arrows denote increase in concentration.

destabilization mechanism. The 2 wt% NaCas-stabilized nanoemulsion behaved in a similar way than the 1 wt% nanoemulsion but flocculation kinetics was slower (data not shown). Nanoemulsions behaved in a different way than conventional emulsions with similar formulations. When NaCas concentrations were low (1–2 wt%), conventional emulsions destabilized mainly by creaming of individual particles (Álvarez Cerimedo et al., 2010). Due to the reduction in droplets size, gravitational force did not affect individual particles stability, and therefore, despite the low protein content, the main destabilization mechanisms involved aggregation: sedimentation of protein aggregates or flocculation of oil droplets. For the nanoemulsion formulated with 4 wt% NaCas and without sucrose no significant changes were detected for 2 months, indicating the great stability of this nanoemulsion (Fig. 5c). Conventional emulsions with protein concentrations around 4 wt% destabilized by flocculation in a week. There is no way to enhance stability of conventional systems without sucrose (Álvarez Cerimedo et al., 2010). Nanoemulsions, however, were very stable with a more simple formulation and there was no need of additives in the aqueous phase to enhance stability. The nanoemulsion with 4 wt% NaCas and 8 wt% sucrose showed no significant changes in 2 months and was as stable as the formulation without sucrose. The 3 wt% NaCas-stabilized nanoemulsion showed a similar behavior than the 4 wt% NaCas nanoemulsion (data not shown). The differences in stability behavior between nano and conventional emulsions were most likely due to differences in droplets sizes. Due to the smaller sizes obtained for addition of evaporative step to processing method, gravitational forces effect on individual particles were negligible and no creaming destabilization was detected.

3.4. Nanoemulsions structure by CLSM

Fig. 6 shows representative images of CLSM for nanoemulsions formulated without sucrose and with different concentrations of NaCas. For 1 or 2 wt% (Fig. 6a and b, respectively), a few big droplets may be observed. However, most of the droplets had nanosizes. Nanoemulsions with 3 or 4 wt% NaCas did not contain droplets in the conventional emulsions range. Lipid phase looked as a continuous red carpet because droplets sizes were below CLSM sensitivity. Fig. 6 proves that after evaporative step droplet sizes were reduced compared to the ones re-

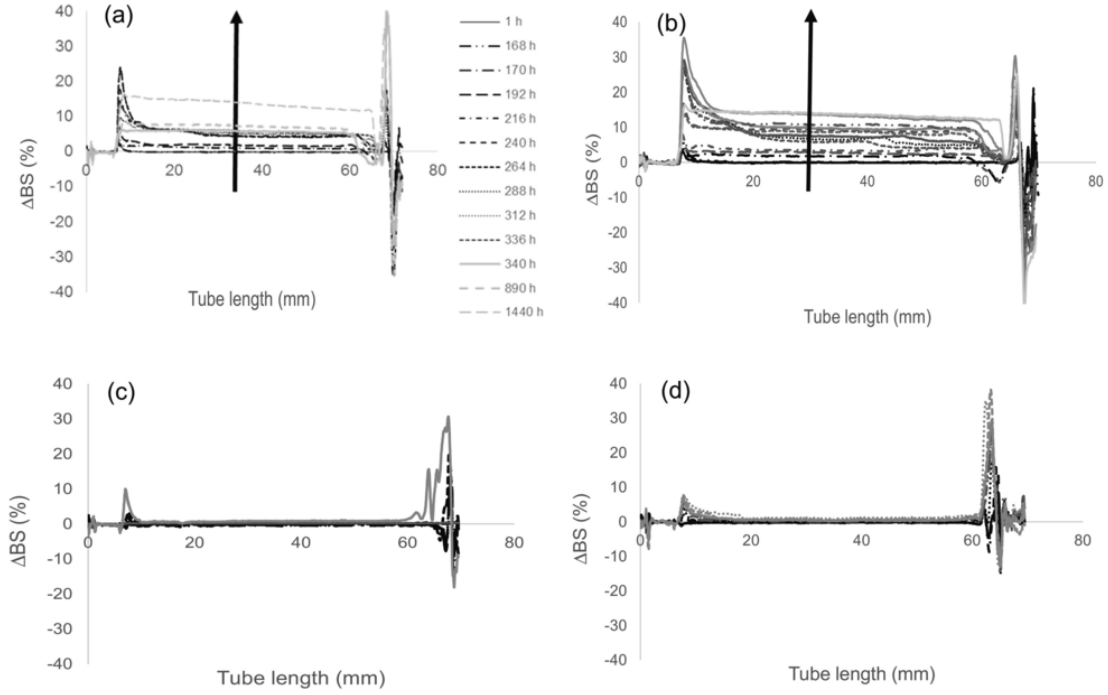

Fig. 5. Back scattering profiles in reference mode (ΔBS) vs. sample height with storage time (samples were stored for 2 months, arrows denote time) in quiescent conditions for emulsions formulated with: (a) 1.0 wt% sodium caseinate (NaCas) and no sucrose added; (b) 1.0 wt% NaCas and 8 wt% sucrose; (c) 4.0 wt% NaCas and no sucrose added; (d) 4.0 wt% NaCas and 8 wt% sucrose. Tube length 65 mm.

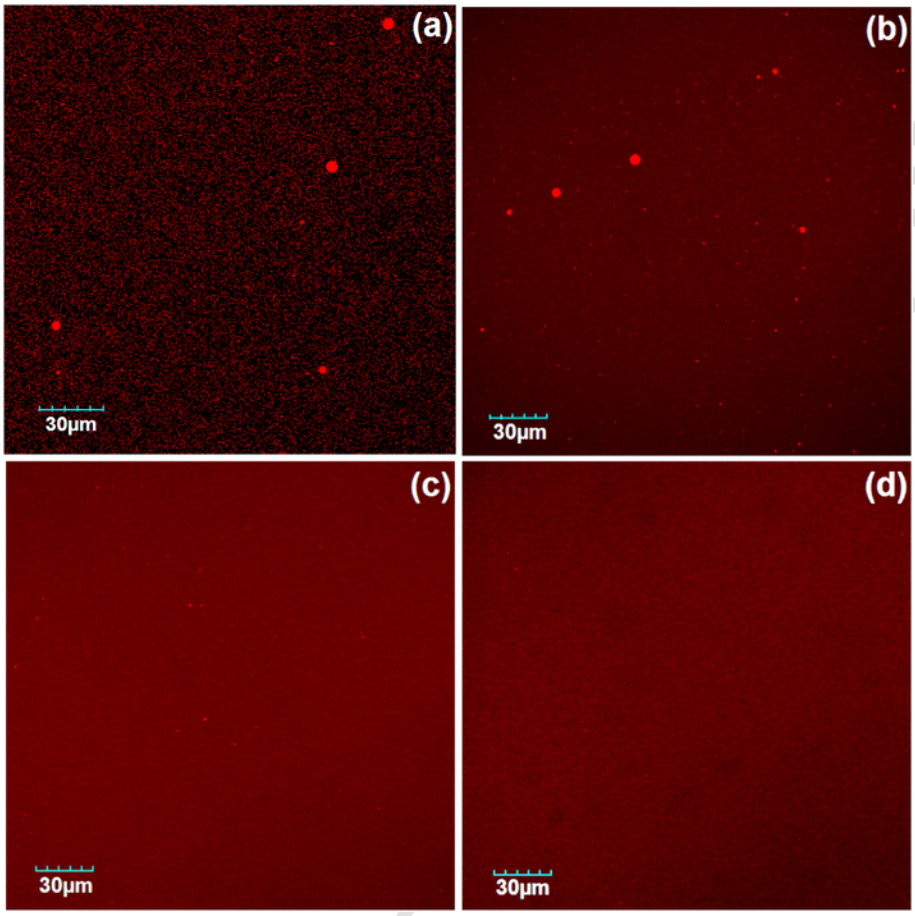

Fig. 6. Confocal laser scanning microscopy (CLSM) images of nanoemulsions formulated without sucrose and different concentrations of NaCas: (a) 1 wt%, (b) 2 wt%, (c) 3 wt%, (d) 4 wt%.

ported for conventional emulsions (Álvarez Cerimedo et al., 2010). Nanoemulsions containing 4 wt% NaCas and different concentrations of sucrose also had droplets in the nano range (data not shown). Droplets in the conventional emulsion range did not appear in these samples.

3.5. Nanoemulsions structure by SAXS

Fig. 7 shows normalized intensity vs. q curves for nanoemulsions formulated without sucrose (Fig. 7a) and for nanoemulsions with 4 wt% NaCas and different sucrose concentrations (Fig. 7b).Values of q_{max} of peaks in curves shown in Fig. 7 were summarized in Table 4. The peak at lower q was most likely due to the contribution of oil droplets surrounded by protein molecules while the peak at higher q was mainly due to interactions among casein micelles. The first peak was not noticeable in conventional emulsions (Huck Iriart et al., 2016). In those systems, oil droplets were too big to be detected by SAXS. Nanoemulsions formulated with 1 or 2 wt% NaCas showed only one peak associated to casein micelles interactions. They did not have a contribution at lower q value indicating that droplets had greater diameter or were aggregated (Fig. 7a, Table 4). In agreement with confocal im-

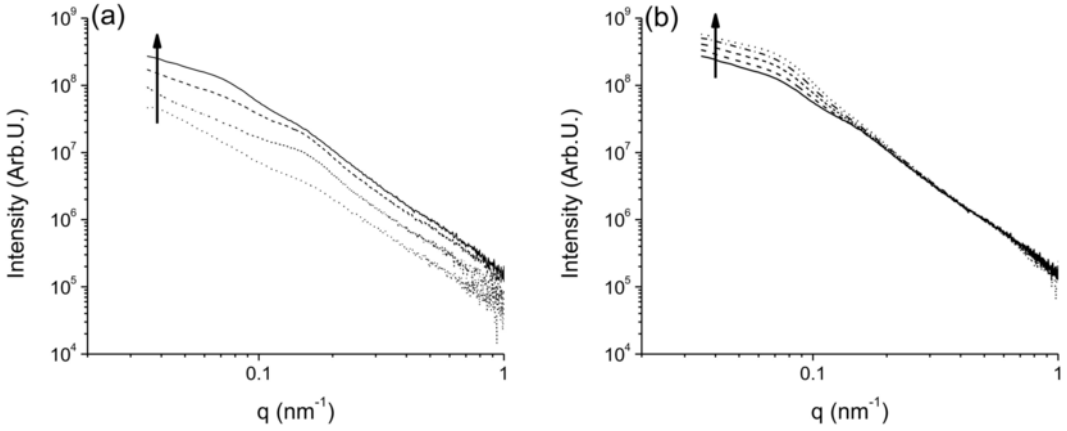

Fig. 7. Normalized intensity vs. scattering vector q for nanoemulsions formulated with (a) (· · ·) 1%, (···) 2%, (- - -) 3%, (–) 4 wt% NaCas, without addition of sucrose; (b) 4 wt% NaCas and (–) 0%, (- - -) 2%, (···) 4%, (- · - ·) 6%, and (· · ·) 8 wt% sucrose. Arrows indicate: (a) increasing caseinate concentration, (b) increasing sucrose concentration.

Table 4
Maximum scattering vector (q_{max}) corresponding to peaks of normalized intensity vs. q curves reported in Fig. 7.

Nanoemulsion	q_{1max} (nm^{-1})	q_{2max} (nm^{-1})
NaCas		
1 wt%		0.17
2 wt%		0.16
3 wt%	0.070	0.16
4 wt%	0.072	0.16
NaCas 4 wt% sucrose		
2 wt%	0.073	0.16
4 wt%	0.073	0.17
6 wt%	0.073	
8 wt%	0.073	

Graphical abstract

ages (Fig. 6), the nanoemulsions that did not contain big droplets had a peak between 0.070 and 0.073 nm^{-1} (lower q) indicating no or very small aggregation of oil droplets. The peak with a q value between 0.16 and 0.17 nm^{-1} was present for all NaCas concentrations (Table 4). This peak was still noticeable up to 4 wt% sucrose concentration. For higher amounts of sucrose, casein micelles correlation was lost (Fig. 7b, Table 4). Interactions between sucrose and casein molecules led to loss of protein ability to aggregate. However, the nanoemulsion formulated with 4 wt% NaCas was stable with or without sucrose addition (Fig. 5). Even with no sucrose added, interactions among casein micelles were not strong enough to destabilize it by flocculation and therefore, the 4 wt% NaCas nanoemulsion remained stable for a long time.

4. Conclusions

Nanoemulsions were successfully prepared by a combination of a high-energy homogenization and evaporative ripening methods. This three-step method allowed obtaining droplet sizes smaller than 120 nm. Stability behavior of NaCas-stabilized nanoemulsions was very dependent on droplets sizes. Systems with droplets smaller than 120 nm behaved in a different way of nanoemulsions prepared by a two-step method or than conventional emulsions. Because droplets sizes were smaller than the ones obtained by high-energy methods, gravitational forces on individual particles were negligible and destabilization by creaming was not noticeable. Selecting a protein concentration at which droplets aggregates were too small to interact to each other, flocculation may be avoided for a long time, even without addition of a co-adjuvant such as sucrose. The 4 wt% NaCas-stabilized nanoemulsion was stable without sugar in the aqueous phase. The third step added to processing method led to the preparation of stable systems with a more simple formulation.

Acknowledgements

This work was supported by the National Agency for the Promotion of Science and Technology (ANPCyT) through Project PICT-2013-0897, and by the University of Buenos Aires through Project UBA-20020130100136BA. The authors wish to thank the Synchrotron Light National Laboratory (LNLS, Campinas, Brazil) for the use of the SAXS1 facilities through proposal 20150056.

References

Álvarez Cerimedo, M.S., Huck Iriart, C., Candal, R.J., Herrera, M.L., 2010. Stability of emulsions formulated with high concentrations of sodium caseinate and trehalose. Food Research International 43, 1482–1493.

Atrux-Tallau, N., Lasselin, J., Han, S.H., Delmas, T., Bibette, J., 2014. Quantitative analysis of ligand effects on bioefficacy of nanoemulsion encapsulating depigmenting active. Colloids and Surfaces B: Biointerfaces 122, 390–395.

Cavalcanti, L.P., Torriani, I.L., Plivelic, T.S., Oliveira, C.L.P., Kellermann, G., Neuenschwander, R., 2004. Two new sealed sample cells for small-angle X-ray scattering from macromolecules in solution and complex fluids using synchrotron radiation. Review of Scientific Instruments 75, 4541–4546.

Chu, B.S., Ichikawa, S., Kanafusa, S., Nakajima, M., 2007. Preparation of protein-stabilized β-carotene nanodispersions by emulsification-evaporation method. Journal of the American Oil Chemists' Society 84, 1053–1062.

Fryd, M.M., Mason, T.G., 2012. Advanced nanoemulsions. Annual Review of Physical Chemistry 63, 493–518.

Gulotta, A., Saberi, A.H., Nicoli, M.C., McClements, D.J., 2014. Nanoemulsion-based deliverysystems for polyunsaturated (ω − 3) oils: Formation using a spontaneous emulsification method. Journal of Agricultural and Food Chemistry 62, 1720–1725.

Hategekimana, J., Chamba, M.V.M., Shoemaker, C.F., Majeed, H., Zhong, F., 2015. Vitamin E nanoemulsions by emulsion phase inversion: Effect of environmental stress and long-term storage on stability and degradation in different carrier oil types. Colloids and Surfaces A: Physicochemical and Engineering Aspects 483, 70–80.

Huck Iriart, C., Montes de Oca Avalos, J.M., Herrera, M.L., Candal, R.J., Pinto de Oliveira, C.L., Linares Torriani, I., 2016. New insights about flocculation process in sodium caseinate-stabilized emulsions. Food Research International 89, 338–346.

Komaiko, J., Sastrosubroto, A., McClements, D.J., 2016. Encapsulation of ω − 3 fatty acids in nanoemulsion-based delivery systems fabricated from natural emulsifiers: Sunflower phospholipids. Food Chemistry 203, 331–339.

Komaiko, J.S., McClements, D.J., 2016. Formation of food-grade nanoemulsions using low-energy preparation methods: A review of available methods. Comprehensive Reviews in Food Science and Safety 15, 331–352.

Lee, S.J., McClements, D.J., 2010. Fabrication of protein-stabilized nanoemulsions using a combined homogenization and amphiphilic solvent dissolution/evaporation approach. Food Hydrocolloids 24, 560–569.

Maher, P.G., Fenelon, M.A., Zhou, Y., Haque, M.K., Roos, Y.H., 2011. Optimization of β-casein stabilized nanoemulsions using experimental mixture design. Journal of Food Science 76, C1108–C1117.

McClements, D.J., 2012. Edible delivery systems for nutraceuticals: Designing functional foods for improved health. Therapeutic Delivery 3, 801–803.

McClements, D.J., 2012. Nanoemulsions versus microemulsions: Terminology, differences, and similarities. Soft Matter 8, 1719–1729.

McClements, D.J., Rao, J., 2011. Food-grade nanoemulsions: Formulation, fabrication, properties, performance, biological fate, and potential toxicity. Critical Reviews in Food Science and Nutrition 51, 285–330.

Mengual, O., Meunier, G., Cayre, I., Puech, K., Snabre, P., 1999. Characterisation of instability of concentrated dispersions by a new optical analyser: The Turbiscan MA 1000. Colloids and Surfaces A: Physicochemical and Engineering Aspects 152, 111–123.

Ozturk, B., Argin, S., Ozilgen, M., McClements, D.J., 2015. Formation and stabilization of nanoemulsion-based vitamin E delivery systems using natural biopolymers: Whey protein isolate and gum arabic. Food Chemistry 188, 256–263.

Pan, L.G., Tomás, M.C., Añón, M.C., 2002. Effect of sunflower lecithins on the stability of water-in-oil and oil-in-water emulsions. Journal of Surfactants and Detergents 5, 135–143.

Rao, J., McClements, D.J., 2013. Optimization of lipid nanoparticle formation for beverage applications: Influence of oil type, cosolvents, and cosurfactants on nanoemulsions properties. Journal of Food Engineering 118, 198–204.

Silva, H.D., Cerqueira, M.A., Vicente, A.A., 2012. Nanoemulsions for food applications: Development and characterization. Food and Bioprocess Technology 5, 854–867.

Tabibiazar, M., Hamishehkar, H., 2015. Formulation of a food grade water-in-oil nanoemulsion: Factors affecting on stability. Pharmaceutical Sciences 21, 220–224.

Thanasukarn, P., Pongsawatmanit, R., McClements, D.J., 2006. Utilization of layer-by-layer interfacial deposition technique to improve freeze-thaw stability of oil-in-water emulsions. Food Research International 39, 721–729.

Troncoso, E., Aguilera, J.M., McClements, D.J., 2012. Fabrication, characterization and lipase digestibility of food-grade nanoemulsions. Food Hydrocolloids 27, 355–363.

Vilanova, N., Solans, C., 2015. Vitamin A palmitate-β-cyclodextrin inclusion complexes: Characterization, protection and emulsification properties. Food Chemistry 175, 529–535.

Yeramilli, M., Ghosh, S., 2017. Long-term stability of sodium caseinate-stabilized nanoemulsions. Journal of Food Science and Technology 54, 82–92.

Zhang, J., Peppard, T.L., Reineccius, G.A., 2015. Preparation and characterization ofnanoemulsions stabilized by food biopolymersusing microfluidization. Flavour and Fragrance Journal 30, 288–294.

Zhang, L., Hayes, D.G., Chen, G., Zhong, Q., 2013. Transparent dispersions of milk-fat-based nanostructured lipid carriers for delivery of β-carotene. Journal of Agricultural and Food Chemistry 61, 9435–9443.